BIOMOLECULES & THERAPEUTICS

**Original Article**
*Biomol Ther 25(4), 427-433 (2017)*

# Galangin Activates the ERK/AKT-Driven Nrf2 Signaling Pathway to Increase the Level of Reduced Glutathione in Human Keratinocytes

**Susara Ruwan Kumara Madduma Hewage, Mei Jing Piao, Kyoung Ah Kang, Yea Seong Ryu, Pattage Madushan Dilhara Jayatissa Fernando, Min Chang Oh, Jeong Eon Park, Kristina Shilnikova, Yu Jin Moon, Dae O Shin and Jin Won Hyun***

*School of Medicine and Institute for Nuclear Science and Technology, Jeju National University, Jeju 63243, Republic of Korea*

## Abstract

Previously, we demonstrated that galangin (3,5,7-trihydroxyflavone) protects human keratinocytes against ultraviolet B (UVB)-induced oxidative damage. In this study, we investigated the effect of galangin on induction of antioxidant enzymes involved in synthesis of reduced glutathione (GSH), and investigated the associated upstream signaling cascades. By activating nuclear factor-erythroid 2-related factor (Nrf2), galangin treatment significantly increased expression of glutamate-cysteine ligase catalytic subunit (GCLC) and glutathione synthetase (GSS). This activation of Nrf2 depended on extracellular signal-regulated kinases (ERKs) and protein kinase B (AKT) signaling. Inhibition of GSH in galangin-treated cells attenuated the protective effect of galangin against the deleterious effects of UVB. Our results reveal that galangin protects human keratinocytes by activating ERK/AKT-Nrf2, leading to elevated expression of GSH-synthesizing enzymes.

**Key Words:** Galangin, Reduced glutathione, Nuclear factor-erythroid 2-related factor, Glutamate-cysteine ligase catalytic subunit, Glutathione synthetase

## INTRODUCTION

Skin health and appearance are both challenged by environmental stress, especially oxidative stress caused by sun exposure (Valacchi *et al*., 2012). The ultraviolet B (UVB; 280-320 nm) and UVA (320-400 nm) spectra are the most destructive wavelengths of solar UV radiation. Exposure to these wavelengths results in production of reactive oxygen species (ROS), which cause oxidative damage to skin cells (Marrot and Meunier, 2008). Cells can counteract the deleterious effects of endogenous or exogenous ROS via the antioxidant defense system, and this protective mechanism can be augmented by natural antioxidants and pharmacological agents (Waster and Ollinger, 2009; Ha *et al*., 2015). Cells respond to these deleterious stimuli in two ways, the early and delayed responses. The early response mechanism involves *in situ* removal of free radicals and ROS via chemical reactions soon after the harmful agents appear (Halliwell, 2007). On the other hand, the delayed response, which is a more sustainable and long-term process, involves expression of genes encoding antioxidant proteins and enzymes that restore the redox balance of the cell (Surh *et al*., 2008). One major target of the delayed response system is nuclear factor-erythroid 2-related factor (Nrf2), which plays a critical role in stress signaling. Nrf2 activates expression of phase II antioxidant enzymes, including glutamate-cysteine ligase catalytic subunit (GCLC) and glutathione synthetase (GSS) (Copple *et al*., 2008; Park and Oh, 2015), which synthesize glutathione (GSH) in both plants and animals (Zhang and Forman, 2012). GSH, which is produced from glutamate, cysteine, and glycine, modulates the activity of thiol-dependent enzymes that are sensitive to redox changes (Filomeni *et al*., 2002).

Many genes that encode antioxidant enzymes have a special nucleotide sequence in their promoter region, the antioxidant responsive element (ARE) (Harvey *et al*., 2009). Nrf2 is a basic leucine zipper protein that detects oxidative stress based on the cell's redox status. Acting as a transcription factor, activated (phosphorylated) Nrf2 binds to the ARE in promoters of antioxidant genes, including those encoding GCLC and GSS, and increases their transcription (Nioi *et al*., 2003).

**Open Access** **https://doi.org/10.4062/biomolther.2016.112**



**Received** May 22, 2016 **Revised** Jul 22, 2016 **Accepted** Aug 2, 2016
**Published Online** Nov 8, 2016

***Corresponding Author**
E-mail: jinwonh@jejunu.ac.kr
Tel: +82-64-754-3838, Fax: +82-64-702-2687

Under normal redox conditions, Nrf2 is maintained in an inactive state in the cytosol, where it is tethered to Kelch-like ECH-associated protein 1 (Keap1). The Keap1 association drives ubiquitination, and ultimately proteasomal degradation, of Nrf2 (Itoh *et al*., 1999). However, oxidative stress stimuli result in cleavage of the Keap1-Nrf2 complex, allowing Nrf2 to accumulate in nucleus, where it binds AREs in the promoters of antioxidant genes (Nioi *et al*., 2003).

Galangin (3,5,7-trihydroxyflavone), a flavonoid abundant in *Alpinia officinarum* and *Helichrysum aureonitens* (Itoh *et al*., 1999; Ciolino and Yeh, 1999), has antibacterial, antiviral, and anticancer properties (Afolayan and Meyer, 1997; Cushnie and Lamb, 2006). In a previous study, we demonstrated that galangin attenuates oxidative DNA damage, lipid and protein oxidation, and expression of apoptotic proteins in human keratinocytes under UVB-induced oxidative stress (Madduma Hewage *et al*., 2015). It remained unclear, however, how galangin interacts with cellular antioxidant defense mechanisms and augments cellular defenses. In this study, we investigated whether galangin affects cellular GSH formation in human keratinocytes via activation of Nrf2.

## MATERIALS AND METHODS

### Reagents

Galangin (3,5,7-trihydroxyflavone) and primary antibodies against ERK, phospho-ERK, GCLC, and GSS were purchased from Santa Cruz Biotechnology (Dallas, TX, USA). 3-(4,5-Dimethylthiazol-2-yl)-2,5-diphenyltetrazolium bromide (MTT) and primary antibody against actin were purchased from Sigma-Aldrich Chemical Company (St. Louis, MO, USA). Buthioninesulfoximine (BSO) was purchased from Cayman Chemical (Ann Arbor, MI, USA). Primary antibodies against TATA-binding protein (TBP) and phospho-Nrf2 were purchased from Abcam (Cambridge, MA, USA). Primary antibodies against Nrf2, AKT, and phospho-AKT were purchased from Cell Signaling Technology (Beverly, MA, USA). Cell Tracker™ Blue CMAC was purchased from Molecular Probes (Eugene, OR, USA). All other chemicals and reagents were of analytical grade.

### Cell culture

HaCaT human keratinocyte cells were purchased from Amore Pacific Company (Yongin, Korea). Cells were maintained at 37°C in an incubator with a humidified atmosphere of 5% $CO_2$ and 95% air. Culture medium was RPMI 1640 containing 10% fetal bovine serum, streptomycin (100 μg/ml), and penicillin (100 units/ml).

### Reverse transcription-PCR (RT-PCR)

Total cellular RNA was isolated using the easy-BLUE™ total RNA extraction kit (iNtRON Biotechnology Inc., Seongnam, Korea). cDNA was amplified using specific primers, 1 μl of RT reaction buffer, dNTPs, and 0.5 U of Taq DNA polymerase in a final volume of 20 μl. PCR conditions were as follows: initial denaturation at 94°C for 5 min; 26 cycles of 94°C for 30 sec, 63°C for 45 sec, 72°C for 1 min; and a final elongation step at 72°C for 10 min. Primer sequences were as follows: GCLC, forward (5′-AACCAAGCGCCATGCCGACC-3′) and reverse (5′-CCTCCTTCCGGCGTTTTCGC-3′); GSS, forward (5′-GCCCCATTCACGCTCTTCCCC-3′) and reverse (5′-ATGCCCGGCCTGCTTAGCTC-3′); GAPDH, forward (5′-TCAAGTGGGGCGATGCTGGC-3′) and reverse (5′-TGCCAGCCCCAGCGTCAAAG-3′). PCR products were mixed with blue/orange 6× loading dye and separated by electrophoresis in a 1% agarose gel and stained with RedSafe™ nucleic acid staining solution (iNtRON Biotechnology Inc.). Gel images were acquired under UV illumination using the Image Quant™ TL analysis software (Amersham Biosciences, Uppsala, Sweden).

### Western blot analysis

Cells were harvested by scraping and lysed using PRO-PREP™ protein extraction solution (iNtRON Biotechnology Inc.). The resultant lysates were centrifuged at 13,000 rpm for 12 min. Supernatants were pipetted into new tubes, and protein concentrations were determined and equalized across samples by addition of suitable volumes of 6×SDS loading dye and PBS. Aliquots were boiled for 5 min and electrophoresed on 10% or 12% SDS-polyacrylamide gels. Protein blots of the gels were transferred onto nitrocellulose membranes, which were blocked with 2% FBS and then incubated with the appropriate primary antibodies (1:1000). Membranes were incubated with horseradish peroxidase-conjugated anti-IgG secondary antibodies (1:5000), and protein bands were detected using enhanced chemiluminescence Western blotting detection kit (Amersham Biosciences).

### Immunocytochemistry

Cells were seeded in 4-well chamber slides at a density of $1.0\times10^5$ cells/ml. After incubation for about 20 h, cells were treated with 40 μM galangin for an additional 6 h. Subsequently, cells were fixed with 1% paraformaldehyde for 30 min, and then washed three times with PBS (5 min each). Fixed cells were permeabilized with PBS containing 1% Triton X-100 for 30 min, and then washed with PBS. Cells were blocked with PBS containing 5% bovine serum albumin for 1 h at 37°C, and then incubated overnight with anti-Nrf2 antibody diluted in blocking medium (1:100). To visualize the anti-Nrf2 antibody, cells were treated with FITC-conjugated secondary antibody (1:500) for 2 h. After washing with PBS, stained cells were mounted onto microscope slides in mounting medium containing DAPI (Vector, Burlingame, CA, USA). Images were collected on a Zeiss confocal microscope using the LSM 510 software (Carl Zeiss, Jena, Germany).

### GSH assay

GSH level was assessed by confocal microscopy. Cells were seeded in 4-well chamber slides at a density of $1\times10^5$ cells/ml. Sixteen hours after seeding, cells were treated with 40 μM galangin, incubated for 1 h, and then exposed to a UVB dose of 30 mJ/cm$^2$. After 24 h, 10 μM CMAC staining dye was added to each well, and the samples were incubated for an additional 30 min at 37°C. After washing with PBS, the stained cells were mounted on a chamber slide in mounting medium. Images were collected on a confocal microscope using the LSM 5 PASCAL software. In addition, GSH concentration was measured using the BIOXYTECH GSH-400 assay kit (Foster City, CA, USA).

### Cell viability assay

Cells were seeded in 24-well plates at a density of $1\times10^5$ cells/ml. BSO was added to a final concentration of 100 μM, and the cells were incubated for 1 h. Galangin was added at a

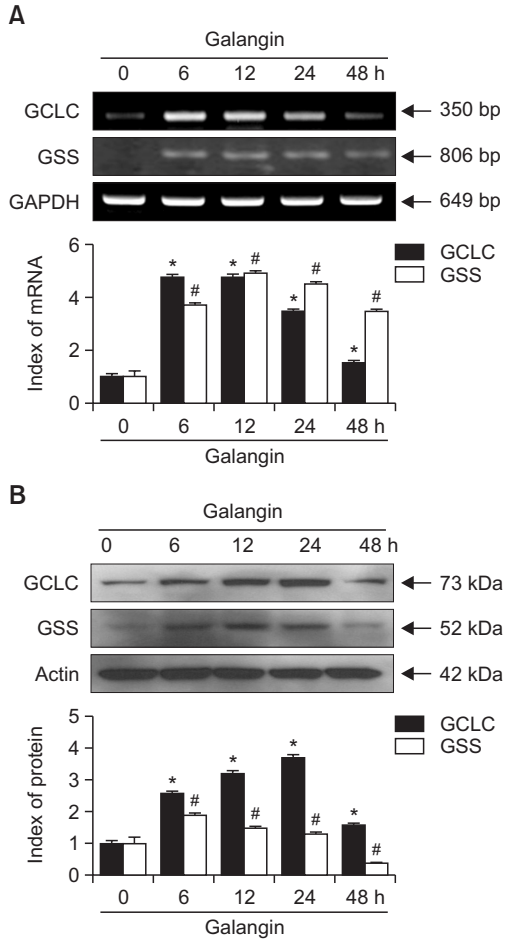


**Fig. 1.** Effect of galangin on GCLC and GSS expression in HaCaT cells. (A) Cells were treated with 40 μM galangin and incubated for up to 48 h. After harvest, cells were subjected to (A) RT-PCR and (B) Western blot to analyze GCLC and GSS mRNA and protein levels. *,#Significantly different from control of GCLC and GSS, respectively ($p$<0.05).

final concentration of 40 μM, and the cells were incubated for an additional hour. The cells were then exposed to UVB and incubated for 24 h. MTT stock solution was added to each well to yield a final reaction volume of 500 μl. The supernatant was aspirated 4 h later, and formazan crystals were dissolved in 500 μl of dimethyl sulfoxide (DMSO). Absorbance at 540 nm was measured using a scanning multi-well spectrophotometer.

### Statistical analysis

All measurements were performed in triplicate, and all values are expressed as means ± standard error. The results were subjected to analysis of variance followed by Tukey's test to determine differences between means. In each case, a $p$-value less than 0.05 was considered statistically significant.

## RESULTS

### Galangin upregulates the expression of GCLC and GSS mRNA and protein

In a previous study, we showed that 40 μM galangin efficiently scavenges UVB-induced ROS, attenuates macromolecular damage, and diminishes the expression of apoptotic proteins (Madduma Hewage *et al*., 2015). Accordingly, we used the same concentration of galangin for this experiment. HaCaT cells were treated with 40 μM galangin and incubated

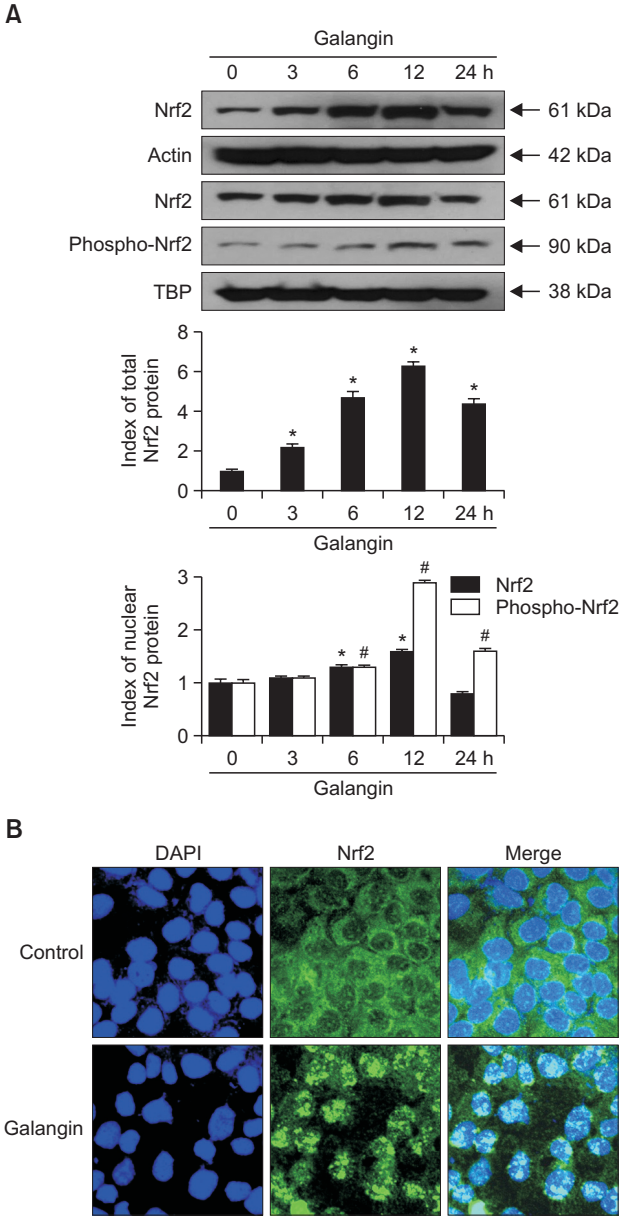


**Fig. 2.** Effect of galangin on expression and nuclear translocation of Nrf2. Whole cell lysate and nuclear fractions of HaCaT cells were extracted following treatment with galangin (40 μM) and incubated for 24 h. (A) Western blots were performed using antibody against Nrf2 and phospho-Nrf2. *,#Significantly different from control of Nrf2 and phospho-Nrf2, respectively ($p$<0.05). (B) Nrf2 translocation to the nucleus was assessed by immunocytochemistry. An anti-Nrf2 antibody and a FITC-conjugated secondary antibody were used to detect Nrf2 localization (green) using confocal microscopy. DAPI staining indicates the locations of nuclei (blue). The merged images show the subcellular localization of the Nrf2 protein.

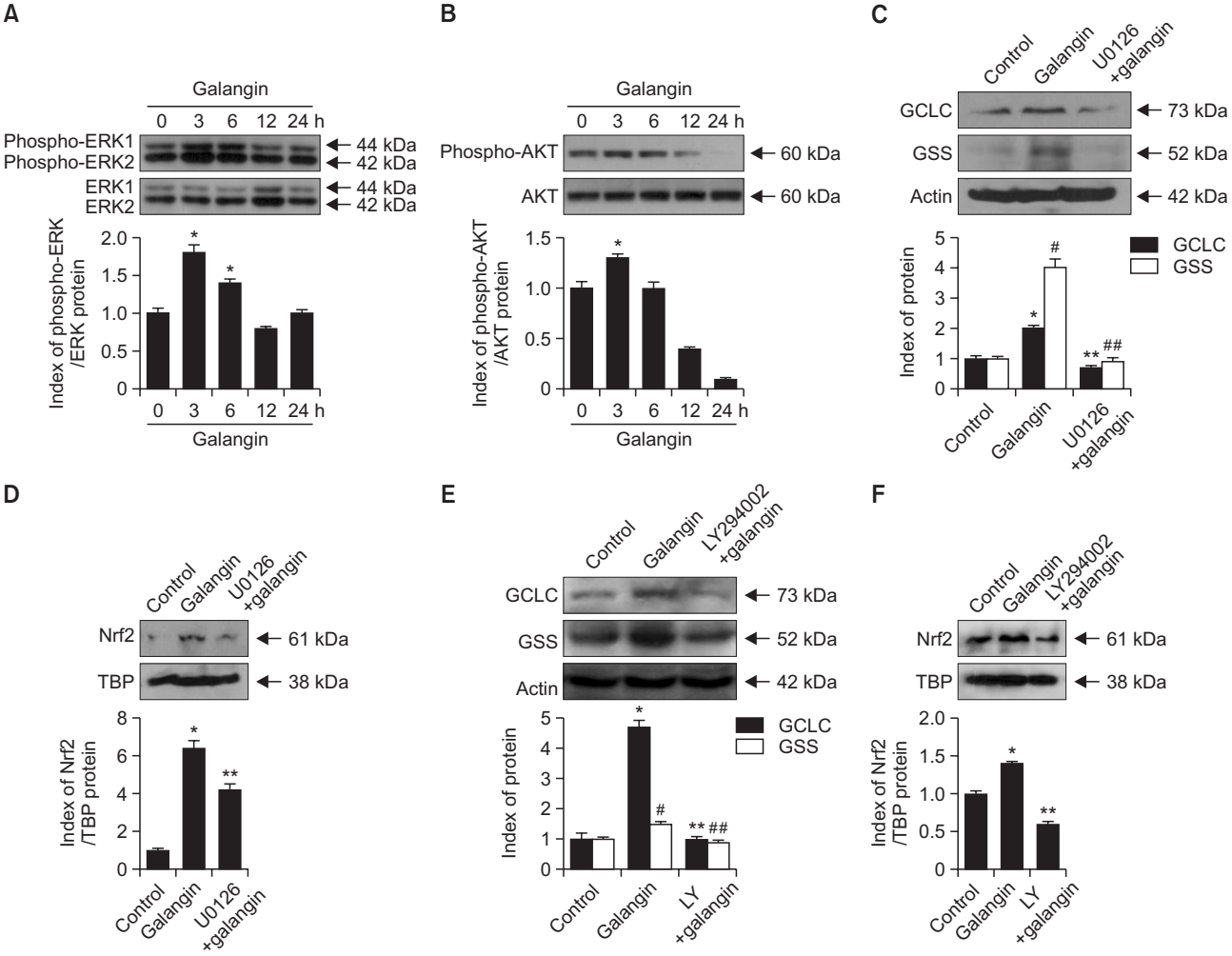


**Fig. 3.** Effect of galangin on ERK and AKT signaling. Cells treated with 40 μM galangin were harvested at different incubation periods (0-24 h) and subjected to Western blot analysis using primary antibodies against (A) phospho-ERK1/2 and ERK1/2, and (B) phospho-AKT and AKT. *Significantly different from control ($p$<0.05). Prior to galangin treatment, cells were treated with U0126 or LY294002. Western blot was performed to (C, E) GCLC and GSS expression and (D, F) Nrf2 level. (C, E) *,#Significantly different from control of GCLC and GSS, respectively ($p$<0.05). **,##Significantly different from control of galangin-treated GCLC and GSS, respectively ($p$<0.05). (D, F) *,** Indicate significant differences from control and galangin-treated cells ($p$<0.05).

for up to 48 h, and the levels of GCLC and GSS mRNA and protein were monitored. RT-PCR was performed to measure mRNA levels. Expression of both GCLC and GSS mRNAs was elevated (Fig. 1A). Western blot analysis confirmed that the levels of both proteins mirrored the corresponding mRNA levels (Fig. 1B). These observations clearly show that galangin significantly increases the expression of GCLC and GSS in HaCaT cells, at both the mRNA and protein levels.

## Galangin stimulates Nrf2 activation

Nrf2 is the main transcription factor responsible for GCLC and GSS expression under oxidative stress. Therefore, we examined Nrf2 activation and nuclear translocation by both Western blot and immunocytochemistry. As shown in Western blot result, galangin remarkably enhanced the expression of Nrf2 in the whole cell lysate and phosphorylation of nuclear Nrf2 (active form) (Fig. 2A). These results were confirmed by confocal microscopy with Nrf2-specific antibodies: galangin-treated cells contained higher levels of nuclear Nrf2 than control cells (Fig. 2B). These results showed that galangin promotes nuclear translocation and activation of Nrf2.

## Galangin-induced Nrf2 activation is governed by phosphorylation of ERK and AKT

Generally, Nrf2 activation is affected by its upstream signaling network of extracellular signal-regulated kinases (ERKs) and protein kinase B (AKT) (Papaiahgari *et al*., 2006). To determine the roles of these proteins in the effects of galangin, we analyzed ERK and AKT expression in response to galangin treatment for up to 24 h. Both ERK and AKT were phosphorylated (i.e., activated) within 6 h of galangin treatment, consistent with the idea that activation of Nrf2 by galangin is mediated by ERK and AKT (Fig. 3A, 3B). Next, we examined the effect of U0126 and LY294002, which are specific inhibitors of ERK and AKT, respectively, on GCLC and GSS expression in galangin-treated cells. Pretreatment with ERK and AKT inhibi-

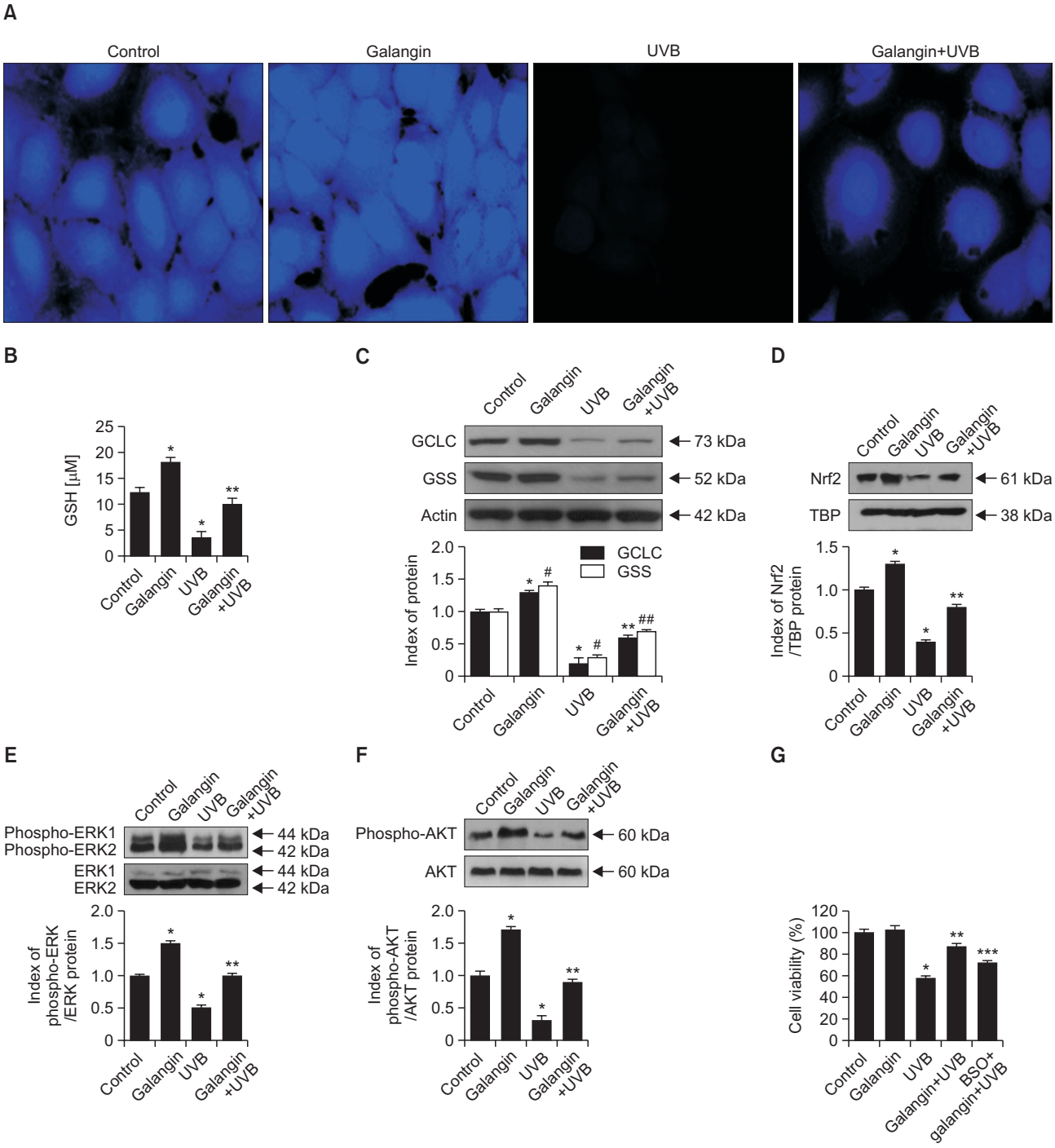


**Fig. 4.** Influence of galangin on the GSH level in HaCaT cells. Cells were plated in 4-well chamber slides, incubated for 16 h, treated with galangin for 1 h, exposed to UVB, and incubated for an additional 24 h. (A) Cells were stained with GSH specific-staining dye CMAC and observed under confocal microscopy. (B) GSH level in HaCaT cells was quantitated using a commercial GSH assay kit. *,** indicate significant differences from control and UVB-treated cells, respectively ($p$<0.05). Cells were treated with galangin, incubated for additional 1 h and exposed to UVB. Cell lysates were subjected to western blot analysis to measure the (C) GCLC and GSS expression, (D) nuclear Nrf2 expression, (E) ERK1/2 and (F) AKT phosphorylation. (C) *,#Significantly different from control of GCLC and GSS, respectively ($p$<0.05). **,##Significantly different from GCLC and GSS of UVB-treated cells, respectively ($p$<0.05). (D-F) *,** Indicate significant differences from control and UVB-treated cells ($p$<0.05). (G) Cells were pretreated with BSO to investigate the significance of GSH in galangin-induced protection of human keratinocytes against oxidative stress. *,**,*** Indicate significant differences from control, UVB-treated cells, and galangin+UVB-treated cells, respectively ($p$<0.05).

tors dramatically reduced the induction of GCLC and GSS by galangin treatment (Fig. 3C, 3E). Also, Nrf2 levels induced by galangin were significantly decreased in the presence of ERK and AKT inhibitors, respectively (Fig. 3D, 3F). Together, these results confirm that galangin-induced GCLC and GSS expression is controlled by ERK- and AKT-mediated Nrf2 activation.

### Galangin increases GSH synthesis and protects HaCaT cells against oxidative damage

GSH is the most abundant antioxidant in both plants and animals, and it makes a vital contribution to cellular antioxidant defense (Zhang and Forman, 2012). To investigate the importance of GSH in the effects of galangin, we treated cells with 40 μM galangin, exposed them to UVB, and evaluated the GSH level using confocal microscopy and a commercial GSH assay kit. In Fig. 4A, the intensity of blue fluorescence in the confocal microscopic images indicates the GSH level. Galangin treatment increased the GSH level in UVB non-treated cells, and partially restored the reduced GSH level following UVB exposure (Fig. 4A, 4B). Because GSH synthesis is catalyzed by GCLC and GSS, we examined the levels of these enzymes in UVB-exposed cells. UVB exposure markedly attenuated the expression of both GCLC and GSS, but pretreatment of galangin diminished the reduction in both proteins (Fig. 4C). Since galangin was able to recover the UVB-induced GSH depletion, we next studied the effect of galangin on the expression of Nrf2 as well as ERK and AKT in UVB-irradiated keratinocytes. As shown in Fig. 4D, decrease of Nrf2 by UVB was significantly recovered by the galangin. Consistent with these data, galangin notably recovered the phosphorylated ERK and AKT decreased by UVB (Fig. 4E, 4F). BSO is an inhibitor of glutamylcysteine synthetase that lowers the GSH level (Drew and Miners, 1984). To determine whether the protective effect of galangin against UVB-induced oxidative stress is mediated by GSH, we assessed cell viability following UVB exposure. UVB exposure decreased cell viability to 55%, which was increased to 85% by galangin pretreatment; however, only 70% of cells pretreated with both BSO and galangin were viable (Fig. 4G). These results confirm that galangin protects cells against oxidative stress in part by inducing production of GSH.

## DISCUSSION

As an antioxidant, GSH plays many important roles in biological systems, and it also has various functions in nutrient metabolism, gene expression, and DNA and protein synthesis (Chen *et al*., 2011). GSH is also involved in inhibiting tumor cell growth, preventing apoptosis, and attenuating inflammation (Kudugunti *et al*., 2011; Bolfa *et al*., 2013). GSH is synthesized from glutamate, cysteine, and glycine by the cytosolic enzymes GCLC and GSS (Wu *et al*., 2004). We showed previously that galangin protects human skin keratinocytes from UVB-induced oxidative stress (Madduma Hewage *et al*., 2015). The purpose of this study was to determine whether galangin can elevate GCLC and GSS expression, thereby obtaining cytoprotection through GSH synthesis.

Galangin significantly increased the expression of GCLC and GSS at both the mRNA and protein levels (Fig. 1). Under stress conditions, cytoplasmic Nrf2 is cleaved from the Keap1-Nrf2 complex, enabling it to translocate into the nucleus where it recognizes and binds AREs in the promoters of genes encoding antioxidant enzymes, thereby inducing their transcription (Jaiswal, 2004). Therefore, we investigated whether Nrf2 is activated in galangin-treated cells. A significant increase of phospho-Nrf2 level in galangin-treated cells was observed in the nuclear fraction (Fig. 2A), which was confirmed by immunocytochemistry (Fig. 2B). Nrf2 activation is facilitated by the ERK and/or AKT pathway (Martin *et al*., 2004; Papaiahgari *et al*., 2006); indeed, galangin significantly increased the phosphorylation of ERK and AKT (Fig. 3A, 3B). To determine whether inhibition of ERK or AKT could affect GCLC or GSS expression, we treated cells with U0126 and LY294002 prior to galangin treatment. Inhibition of ERK and AKT attenuated the induction of GCLC and GSS expression by galangin (Fig. 3C, 3E). Similar effect was observed in the expression of nuclear Nrf2 in the presence of ERK and AKT inhibition (Fig. 3D, 3F) revealing that ERK and AKT signaling are involved in Nrf2 activation.

GSH is oxidized to neutralize ROS generated followed by the UVB exposure; consequently, the GSH level is reduced by UVB treatment. Galangin induces GCLC and GSS expression, and galangin-treated cells contained higher levels of GSH than control cells. Because GCLC and GSS are involved in GSH synthesis, we also measured the levels of both enzymes by Western blotting. Consistent with previous findings, galangin upregulated the expression of GCLC and GSS in both UVB-treated and non-treated cells (Fig. 4C). Further activation of ERK and AKT in UVB-irradiated and non-irradiated cells well established our findings that ERK and AKT signaling are mediated in Nrf2 transcription; simultaneously activate GCLC and GSS protein expressions in human keratinocytes. BSO is an inhibitor of gamma-glutamylcysteine synthetase, and thus an inhibitor of GSH synthesis; we used this compound to investigate the importance of GSH in the protective effect of galangin against UVB-induced oxidative damage. In UVB-exposed cells, galangin treatment decreased the rate of cell death relative to that of only UVB-treated cells. By contrast, cells pretreated with BSO prior to galangin treatment and UVB exposure exhibited increase of the rate of cell death (Fig. 4G).

Together, these results confirm that galangin phosphorylates ERK and AKT to activate Nrf2 nuclear translocation. In the nucleus, Nrf2 binds to the ARE in the promoters of the genes encoding GCLC and GSS, thereby inducing their transcription. Higher levels of GCLC and GSS promote synthesis of GSH, which plays prominent roles in cellular defense, especially against oxidative stress.

## ACKNOWLEDGMENTS

This research was supported by the 2016 scientific promotion program funded by Jeju National University.

## REFERENCES

Afolayan, A. J. and Meyer, J. J. (1997) The antimicrobial activity of 3,5,7-trihydroxyflavoneisolated from the shoots of *Helichrysum aureonitens*. *J. Ethnopharmacol.* **57**, 177-181.

Bolfa, P., Vidrighinescu, R., Petruta, A., Dezmirean, D., Stan, L., Vlase, L., Damiane, G., Catoi, C., Filip, A. and Clichici, S. (2013) Photoprotective effects of *Romanian propolis* on skin of mice exposed to UVB irradiation. *Food Chem. Toxicol.* **62**, 329-342.

Chen, J. S., Huang, P. H., Wang, C. H., Lin, F. Y., Tsai, H. Y., Wu, T. C., Lin, S. J. and Chen, J. W. (2011) Nrf-2 mediated heme oxygenase-1 expression, an antioxidant-independent mechanism, contributes to anti-atherogenesis and vascular protective effects of *Ginkgo biloba* extract. *Atherosclerosis* **214**, 301-309.

Ciolino, H. P. and Yeh, G. C. (1999) The flavonoid galangin is an inhibitor of CYP1A1activity and an agonist/antagonist of the aryl hydrocarbon receptor. *Br. J. Cancer* **79**, 1340-1346.

Copple, I. M., Goldring, C. E., Kitteringham, N. R. and Park, B. K. (2008) The Nrf2-Keap1 defense pathway: role in protection against drug-induced toxicity. *Toxicology* **246**, 24-33.

Cushnie, T. P. and Lamb, A. J. (2006) Assessment of the antibacterial activity of galangin against 4-quinolone resistant strains of *Staphylococcus aureus*. *Phytomedicine* **13**, 187-191.

Drew, R. and Miners, J, O. (1984) The effects of buthionine sulphoximine (BSO) on glutathione depletion and xenobiotic biotransformation. *Biochem. Pharmacol*. **33**, 2989-2994.

Filomeni, G., Rotilio, G. and Ciriolo, M. R. (2002) Cell signalling and the glutathione redox system. *Biochem. Pharmacol.* **64**, 1057-1064.

Ha, B. G., Park, M. A., Lee C. M. and Kim, Y. C. (2015) Antioxidant activity and anti-wrinkle effects of *Aceriphyllum rossii* leaf ethanol extract. *Toxicol. Res*. **31**, 363-369.

Halliwell, B. (2007) Biochemistry of oxidative stress. *Biochem. Soc. Trans.* **35**, 1147-1150.

Harvey, C. J., Thimmulappa, R. K., Singh, A., Blake, D. J., Ling, G., Wakabayashi, N., Fujii, J., Myers, A. and Biswal, S. (2009) Nrf2-regulated glutathione recycling independent of biosynthesis is critical for cell survival during oxidative stress. *Free Radic. Biol. Med.* **46**, 443-453.

Itoh, K., Wakabayashi, N., Katoh, Y., Ishii, T., Igarashi, K., Engel, J. D. and Yamamoto, M. (1999) Keap1 represses nuclear activation of antioxidant responsive elements by Nrf2 through binding to the amino-terminal Neh2 domain. *Genes Dev*. **13**, 76-86.

Jaiswal, A. K. (2004) Nrf2 signaling in coordinated activation of antioxidant gene expression. *Free Radic. Biol. Med*. **36**, 1199-1207.

Kudugunti, S. K., Vad, N. M., Ekogbo, E. and Moridani, M. Y. (2011) Efficacy of caffeic acid phenethyl ester (CAPE) in skin B16-F0 melanoma tumor bearing C57BL/6 mice. *Invest. New Drugs* **29**, 52-62.

Madduma Hewage, S. R., Piao, M. J., Kim, K. C., Cha, J. W., Han, X., Choi, Y. H., Chae, S. and Hyun, J. W. (2015) Galangin (3,5,7-trihydroxyflavone) shields human keratinocytes from ultraviolet B-induced oxidative stress. *Biomol. Ther. (Seoul)* **23**, 165-173.

Marrot, L. and Meunier, J. R. (2008) Skin DNA photodamage and its biological consequences. *J. Am. Acad. Dermatol.* **58**, S139-S148.

Martin, D., Rojo, A. I., Salinas, M., Diaz, R., Gallardo, G., Alam, J., Ruiz de Galarreta, C. M. and Cuadrado, A. (2004) Regulation of heme oxygenase-1 expression through the phosphatidylinositol 3-kinase/Akt pathway and the Nrf2 transcription factor in response to the antioxidant phytochemical carnosol. *J. Biol. Chem*. **279**, 8919-8929.

Nioi, P., McMahon, M., Itoh, K., Yamamoto, M. and Hayes, J. D. (2003) Identification of a novel Nrf2-regulated antioxidant response element (ARE) in the mouse NAD(P)H:quinone oxidoreductase 1 gene: reassessment of the ARE consensus sequence. *Biochem. J*. **374**, 337-348.

Papaiahgari, S., Zhang, Q., Kleeberger, S. R., Cho, H. Y. and Reddy, S. P. (2006) Hyperoxia stimulates an Nrf2-ARE transcriptional response via ROS-EGFR-PI3K-Akt/ERK MAP kinase signaling in pulmonary epithelial cells. *Antioxid. Redox Signal*. **8**, 43-52.

Park, G. and Oh, M. S. (2015) Acceleration of heat shock-induced collagen breakdown in human dermal fibroblasts with knockdown of NF-E2-related factor 2. *BMB Rep*. **48**, 467-472.

Surh, Y. J., Kundu, J. K. and Na, H. K. (2008) Nrf2 as a master redox switch in turning on the cellular signaling involved in the induction of cytoprotective genes by some chemopreventive phytochemicals. *Planta Med*. **74**, 1526-1539.

Valacchi, G., Sticozzi, C., Pecorelli, A., Cervellati, F., Cervellati, C. and Maioli, E. (2012) Cutaneous responses to environmental stressors. *Ann. N. Y. Acad. Sci.* **1271**, 75-81.

Waster, P. K. and Ollinger, K. M. (2009) Redox-dependent translocation of p53 to mitochondria or nucleus in human melanocytes after UVA- and UVB-induced apoptosis. *J. Invest. Dermatol*. **129**, 1769-1781.

Wu, G., Fang, Y. Z., Yang, S., Lupton, J. and Turner, N. D. (2004) Glutathione metabolism and its implications for health. *J. Nutr*. **134**, 489-492.

Zhang, H. and Forman, H. J. (2012) Glutathione synthesis and its role in redox signaling. *Semin. Cell Dev. Biol*. **23**, 722-728.